

# Time-resolved connectivity reveals the “how” and “when” of brain networks reconfiguration during face processing

Antonio Maffei<sup>a</sup>, Paola Sessa<sup>a,b,\*</sup>

<sup>a</sup> Padova Neuroscience Center (PNC), University of Padova, Italy

<sup>b</sup> Department of Developmental and Social Psychology, University of Padova, Italy

## ARTICLE INFO

### Keywords:

Time-varying connectivity  
Face processing  
MEG  
Dynamic networks  
Global efficiency  
Brain entropy

## ABSTRACT

Recent advances in the study of human brain networks suggest that efficient cognitive operations depend on dynamic changes in large-scale connectivity. In this study we used face processing as a probe to shed light into these dynamics, considering that it relies on a set of well-studied brain regions, whose activity has been well detailed in terms of its timing. By modeling cortical connectivity from MEG recordings during the presentation of face and scrambled images, we show that the whole-brain network topology becomes more efficient and complex in response to a face than a scrambled image, in an early time-window with a peak at ~170 ms. We also observed that the *core* and the *extended* systems of the face processing network become topologically closer, in a dynamic readjustment of connectivity weights that maximize the efficiency of their communication. Furthermore, using time-resolved decoding we observed that face familiarity can be distinguished very early on from the functional connectivity. Altogether, these results represent a crucial advancement for understanding of how dynamic reshaping of cortical connectivity supports cognitive processing of complex visual stimuli, and provide critical insights on the dynamic subtending face processing.

## 1. Introduction

In the last years we are witnessing a paradigm shift in functional neuroimaging, with increasing efforts in understanding brain activity in terms of networks and their time-evolving dynamics (Calhoun et al., 2014; Preti et al., 2017). Recent studies have shown that cognitive operations prompt a reshaping of functional connectivity, characterized by increased network integration which is predictive of successful learning in simple visual and motor tasks, although on a slow time-scale (Bassett et al., 2011, 2015). Indeed, these studies relied on connectivity estimated from hemodynamic response collected with f-MRI, which is inherently slow and suboptimal to assess fast dynamics. It is decisive therefore to study the topology of the functional connectome at higher temporal resolution to map its dynamic to the rapid unfolding of cognitive processes. A promising approach is to study functional connectivity estimated from (magneto)-electrophysiological recordings, which allows tracking event-related changes in cortical networks with excellent time precision (Bola and Sabel, 2015; Valencia et al., 2008). Furthermore, it is crucial to quantify how the efficiency of information exchange evolves in time, because that is strictly related with optimal cognitive functioning (Bassett et al., 2009; Santarnecchi et al., 2014). The present

study focused on the whole-brain network dynamical changes during a face perception task, measured with MEG, and seeks to contribute to this goal.

The first question that this research seeks to answer is how the whole-brain network topology changes during a face processing task. Efficient processing depends on a highly integrated network that facilitates information exchange (Bassett et al., 2011; Maffei and Sessa, 2021; Shine et al., 2016). Therefore, we predicted that in response to the presentation of a face the whole-brain network should reconfigure its connections toward a compact and highly efficient topology. Using graph theory, we computed two indices to track these topological changes, namely global efficiency and graph compactness. In addition, we also computed a measure of graph entropy derived from information theory, predicting that if the network undergoes a reshaping, it will consequently carry more information, thus it will be more complex (Lynn et al., 2020; Viol et al., 2017). We predicted to observe an increase in all the three metrics, with a peak of efficiency and complexity within the first 200 ms. Such timing will be coherent with the negative evoked-potential peaking around 170 ms from stimulus onset (i.e., N170/M170) (Eimer, 2012; Rossion, 2014) that is considered to be a “face-sensitive” cortical signature.

\* Corresponding author. Via Venezia 8, 35131, Padova, Italy.

E-mail address: [paola.sessa@unipd.it](mailto:paola.sessa@unipd.it) (P. Sessa).

<https://doi.org/10.1016/j.ynirp.2021.100022>

Received 8 December 2020; Received in revised form 26 May 2021; Accepted 31 May 2021

Available online 6 June 2021

2666-9560/© 2021 The Authors.

Published by Elsevier Inc.

This is an open access article under the CC BY-NC-ND license

(<http://creativecommons.org/licenses/by-nc-nd/4.0/>).

The second question pertains more specifically with the network dynamics that subserve face perception. Face processing has been posited to depend on the activity of several regions organized in two systems: a *core* system, delimited to regions in the extrastriate visual cortex, that code for visual features (both variant and invariant) that define a face as such, and an *extended* system, distributed in frontal, parietal and temporal regions, that code for more abstract dimensions, like identity and emotional expressions (Haxby et al., 2000; Haxby and Gobbini, 2012; Hoffman et al., 2002). Yet, only recently a formal investigation of the topological dynamics of this network has begun (Wang et al., 2020). An important matter of debate is how and when the face perception network extracts abstract features from a face, like its identity. A recent review on the electrophysiological correlates of face familiarity, showed that it can be detected on the scalp starting at 250 ms (Huang et al., 2017). However, it has been recently showed that familiarity information can be extracted very early on ( $\leq 100$  ms), enhancing face processing (Dobs et al., 2019; Ramon and Gobbini, 2018; Visconti di Oleggio Castello and Gobbini, 2015). The hypothesized mechanism is a pattern-matching between the seen face and a template available in memory (Apps and Tsakiris, 2013; Trapp et al., 2018), occurring in the *core* system, exploiting the information back-projected by areas within the *extended* system (Trapp et al., 2018).

In this study, we sought to understand the corresponding network topology dynamics that support the extraction of this information. We measured the dynamic cross-talk between the different nodes of the face perception network, in terms of how information is routed efficiently among them. We hypothesized that this cross-talk will be faster for familiar faces, for which there is a stored memory. On the other hand, for unfamiliar faces we expected to observe a long-lasting information routing between the *core* and the *extended* systems. Furthermore, applying time-resolved decoding on connectivity patterns, we sought to identify the set of connections that best allow the discrimination of a face according to its familiarity.

## 2. Method

### 2.1. Data and preprocessing

In this study we used the open-access dataset published by Wakeman and Henson (2015). The original study consisted in the presentation of a series of images belonging to one of three categories: familiar faces (famous people), unfamiliar faces and phase-scrambled images of a face. The total number of images presented was 300 per each category. Sixteen healthy participants were enrolled in the study, which consisted in viewing the images and answering a question unrelated to the goal of the study (rating the symmetry of the image presented). Brain activity was collected using an Elekta Neuromag VectorView MEG system (102 magnetometers, 204 planar gradiometers), with a 1100 Hz sampling rate. Data were acquired in six 10-min run for a total of 300 trials per stimulus category. Each trial begun with a fixation cross presented on screen for a random duration between 400 and 600 ms, followed by the stimulus which lasted on screen for a random duration between 800 and 1000 ms. For each participant, a structural T1-weighted image was collected from a Siemens 3T TIM TRIO (Siemens, Erlangen, Germany), using an MPRAGE sequence (TR 2250 ms, TE 2.98 ms, TI 900 ms, 190 Hz/pixel; flip angle 9°, voxel resolution = 1 mm). For registration between MEG sensors locations and T1-MRI three fiducial points (nasion, left ear, right ear) were 3-D digitized.

Data preprocessing was performed using a publicly available automatized pipeline developed by the Brainstorm team (Tadel et al., 2019). For each subject and run, preprocessing consisted in the following steps: importing the cortical surface extracted from the T1 MRI using *freesurfer*, co-registering MEG sensor locations with the cortical surface, importing raw MEG recordings, applying a notch filter to remove power-line noise artifact (50 Hz and its harmonics at 100 Hz, 150 Hz and 200 Hz), detection of eye-blink related artifacts and

detection and correction of heartbeat related artifacts using SSP signal projections, marking of any additional segments of the original recordings containing other source of artifacts (i.e. head or body movements, muscle-related artifacts), segmenting the data from  $-500$  ms to 1200 ms after stimulus onset and discarding epochs containing periods previously marked as bad. In order to model source activity, a forward model was first estimated using the three-layer boundary element method (BEM) from OpenMEEG and then an inverse solution was identified using the weighted Minimum Norm Estimation (wMNE) with default parameter. Finally, the resulting inverse solution was down-sampled to the 148 cortical parcels defined in the Destrieux atlas for further analysis, taking the mean activity of the vertices comprised in each parcel. The full dataset can be freely accessed from the OpenNEURO platform (<https://openneuro.org/datasets/ds000117>), and the pre-processing pipeline can be freely accessed as a MATLAB script from [https://github.com/brainstorm-tools/brainstorm3/blob/master/toolbox/script/tutorial\\_frontiers2018\\_single.m](https://github.com/brainstorm-tools/brainstorm3/blob/master/toolbox/script/tutorial_frontiers2018_single.m).

### 2.2. Functional connectivity analysis

Time-resolved functional connectivity was estimated by computing the instantaneous phase-locking value between each pair of cortical regions. For each trial, the signals from each region was first band-pass filtered in the alpha band (8–13 Hz), then the Hilbert transform was applied to derive their analytical representation, and finally the difference in the phase angle across trials between each regions pair was computed according to the formula:

$$PLV(t) = |E [e^{i\Delta\phi(t)}]|$$

where  $\Delta\phi(t)$  represents the relative phase angles between two analytical signals  $z_1(t)$  and  $z_2(t)$  at each time point  $t$ . This strategy resulted in a time-series of weighted undirected functional connectivity matrices that were used for the computation of graph theoretical metrics. This approach has been successfully applied in previous research to characterize time-resolved connectivity from both fMRI (Nobukawa et al., 2019; Pedersen et al., 2018) and M/EEG data (Maffei and Sessa, 2021). The decision to restrict our analysis on alpha band was guided from evidence showing a strong overlap between functional networks estimated with fMRI and networks estimated from alpha oscillations recorded with M/EEG (Mantini et al., 2007; Samogin et al., 2020). Moreover, the activity of large-scale brain networks has a strong relationship with alpha oscillatory activity (Sadaghiani et al., 2010) and phase synchrony in this band mediates the functional integration between cortical regions located to a relative distance from each other (Muller et al., 2018; van Driel et al., 2014). Indeed, slower oscillations ( $< 10$  Hz) are characterized by a topographic spread that recruits the whole cortex, thus informing on the integration processes that occur at very long time scales (Maffei, 2020; Massimini et al., 2004; Steriade et al., 1993). Finally, phase synchrony in the alpha range coordinates gamma oscillations (Bahramisharif et al., 2013), which are related to complex sensory processing (Jerbi et al., 2009; Maffei, 2020; Maffei et al., 2019, 2020) and are thought to be crucially involved in face processing (Rossion, 2014).

In order to control that differences in the phase-based connectivity could not depend on underlying differences in the alpha power (Demuru et al., 2020), we also performed a time-frequency decomposition of the signals for each experimental condition. This decomposition was obtained convolving the source-space signal with a Morlet wavelet (Central frequency = 1 Hz; FWHM = 3 s), and a measure of event-related spectral perturbation (ERS/D) was computed as the percentage of power change compared to the baseline. The TF was computed for the 148 ROIs defined in the Destrieux atlas and considering a baseline of 500 msec to account for edge effects ( $\sim 140$  ms for the alpha band).

### 2.3. Network modeling

In this research we were interested in characterizing what are the time-evolving dynamics governing the topology of the cortical network when it is involved in a complex visual processing task. For this purpose, we focused on three properties, namely network complexity, network efficiency and network diameter. In order to quantify the network complexity, and how it changes in time, we drawn from information theory the concept of Shannon entropy. Shannon entropy is an easy, yet powerful and flexible, statistical measure of the amount of information contained in a signal. A higher information content, thus higher complexity, results in a higher entropy. From a computational perspective, Shannon Entropy of a network  $G$  at time  $t$

$$G_t = \begin{pmatrix} [G]_{1,1} & [G]_{1,2} & \cdots & [G]_{1,b} \\ [G]_{2,1} & [G]_{2,2} & \cdots & [G]_{2,b} \\ \vdots & \vdots & \ddots & \vdots \\ [G]_{a,1} & [G]_{a,2} & \cdots & [G]_{a,b} \end{pmatrix}$$

can be defined as:

$$H_t = - \sum_i^n P(x_i) * \log_2 P(x_i)$$

where  $x_i = [G]_{a,b}$  and  $P(x_i)$  correspond to the probability of observing that connectivity strength among all possible connections in the network.

For what concerns the efficiency and the structure of the network we used instead two metrics derived from graph theory, network diameter and global efficiency. Graph theory is a mathematical framework that allows to easily characterize the behavior of complex systems and represents, *de-facto*, the gold standard for the study of brain networks and its time-dependent properties (Bullmore and Sporns, 2009; Calhoun et al., 2014; Rubinov and Sporns, 2010). Within this framework, a core characteristic of a network is the path length, namely the minimum number of steps needed to connect any pair of nodes in the graph. Starting from this simple property it is possible to define the topology and the efficiency of the information flow in a network. Indeed, a network can be deemed as efficient when information flows rapidly among its nodes, *i.e.* the path length is short. As a consequence, an efficient network is compact. The compactness of a network is described by its diameter, which is simply the longest among all the shortest paths. The smaller its diameter, the more compact is the network and thus connecting any pair of nodes is easier.

Global efficiency is a more fine-grained measure of network efficiency, which is dependent from the inverse of the path length, defined as:

$$E_{glob} = \frac{1}{n(n-1)} \sum_{i \neq j}^n \frac{1}{d(i,j)}$$

where  $n$  is the total number of nodes and  $d(i, j)$  represents the shortest path between node  $i$  and node  $j$ . The global efficiency increases when the path length is short, suggesting that the network has a topological structure that supports an optimal information exchange.

We were interested in modeling the communication between the *core* and the *extended* systems involved in face processing, specifically the portion of the extended system involved in retrieving information pertaining to the knowledge of a face. This goal was accomplished through the following steps. First, we retrieved a meta-analytical map of the activation foci associated with face processing using Neurosynth (Yarkoni et al., 2011). We searched for all the studies included in the Neurosynth database matching the keyword term *face* and extracted the association z-map (FDR correct at  $p < .01$ ). This map encodes, for each voxel, the likelihood of it being activation in the studies matching the query term while not being activated in the studies not matching the query (Yarkoni et al., 2011). Second, we identified using the automated

labeling tools available in AFNI the nodes included in the Destrieux atlas that are activated in response to a face. Finally, we assigned the nodes identified to either the *core* (CS) or the *extended* (ES) system (Fig. 1 and Supplementary Table 1) according to the model described by Haxby and Gobbini (2012); finally, we computed the routing efficiency between the two systems. For this last step, we first computed (at each time point  $t$ ) using the Floyd-Warshall algorithm the whole-network shortest path length matrix  $R_{mat}$ , defined as:

$$R_{mat} = \begin{pmatrix} 1 & \frac{1}{SPL_{1,2}} & \cdots & \frac{1}{SPL_{1,n}} \\ \frac{1}{SPL_{2,1}} & 1 & \cdots & \frac{1}{SPL_{2,n}} \\ \vdots & \vdots & \ddots & \vdots \\ \frac{1}{SPL_{n,1}} & \frac{1}{SPL_{n,2}} & \cdots & 1 \end{pmatrix}$$

in which each off-diagonal entry represents the routing efficiency (*i.e.* the inverse of the shortest path length) between any pair of nodes in the matrix. Then, we defined the routing efficiency between CS and ES as:

$$R_{eff} = \max R_{mat}(CS,ES)$$

which represents the maximum routing efficiency between a node belonging to the CS and a node belonging to the ES. For each metric considered in this study, the analysis was computed for each type of stimulus (familiar face, unfamiliar face, scrambled face) after mean aggregation of adjacent layers in the time-varying network to achieve a final sampling rate of 256 Hz (Taylor et al., 2016) and thresholding each layer to retain the 20% of the strongest connection weights thus mitigating the effect of spurious edges (Maffei and Sessa, 2021). The analyses were performed in MATLAB (v2019a) using custom scripts employing functions from Brainstorm (Tadel et al., 2011) and Brain Connectivity Toolbox (Rubinov and Sporns, 2010).

In order to perform time-resolved decoding of face familiarity, we first vectorized the thresholded connectivity matrices for the Famous and Unfamiliar conditions, and then trained a support vector machine (SVM) classifier using a leave-one-subject out cross-validation scheme (Gi et al., 2018; Grootswagers et al., 2017). At each time point the classifier was trained on the data from a subsample of  $n-1$  subjects, and classification was tested on the remaining data. Time-resolving accuracy was obtained averaging the performance of the decoder across the  $n$  folds for each sampling point. Model weights in the time window in which the decoder performed significantly above chance in the classification task were projected in the connectivity space, after multiplying them with the data covariance, in order to retrieve the edges most important for the classification task (Grootswagers et al., 2017; Haufe et al., 2014). This latter step is necessary to make the weights of multivariate model interpretable. Indeed, the weight matrix acts as a filter to project the observed data (in this case edge strengths) to a latent space that maximizes classification (Haufe et al., 2014). Nevertheless, the actual values of this weight matrix, being a function of both signal and noise in the data, does not allow to draw conclusions on the one-to-one mapping between the latent and the observed features (Haufe et al., 2014). The multiplication of the model weights with the data covariance, reverts this process and make the model weights interpretable, telling, in this case, how much an edge contributes to classification accuracy.

Finally, as an additional control analysis, we computed the correlation between the event-related fields and each network metric time-series. The aim of this analysis was to rule out the possibility that the latter could provide redundant information, and thus event-related network dynamics could reflect simpler dynamics already present in the event-related fields time-series.

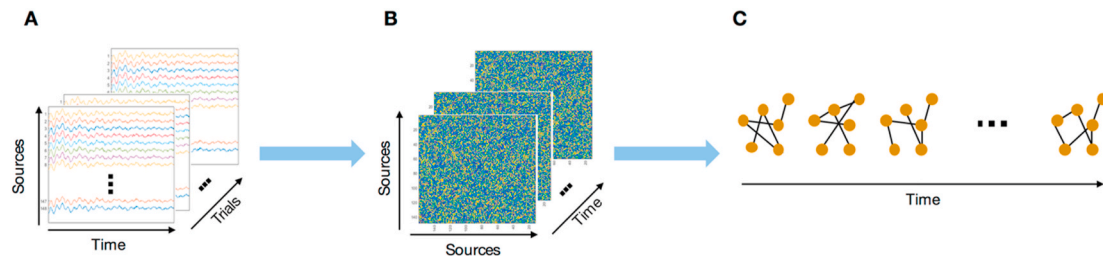


**Fig. 1.** Overview of the analysis scheme. Source activity in response to faces and scrambled images was reconstructed from MEG recordings for each trial (A). Then, time-varying connectivity was estimated using the instantaneous phase-locking value in the alpha band (B). From the time-resolved adjacency matrices, the topology of the network was quantified at each time-point (C).

#### 2.4. Statistical analysis

Statistical modeling was performed within a massive univariate non-parametric permutation framework (Groppe et al., 2011). This approach has been widely accepted in the neuroimaging field because it allows to relax the very strict assumptions of parametric models, which are rarely met, and at the same time allows taking into account the full multidimensional structure of the data without restricting *a-priori* the testing to specific set of regions/sensors and time-window(s) (Maris and Oostenveld, 2007). It consists in performing a statistical test (like a *t*-test or ANOVA) for every point in the region by time plane, then iteratively permuting the within-subject condition assignment and performing the test a sufficient number of times to construct an empirical distribution of the test statistic under the null hypothesis that the condition labels are interchangeable. This empirical null-distribution is then used to derive the exact probability and perform the statistical inference (Maris and Oostenveld, 2007).

For each metric we had a time series per each subject and stimulus category, that were used to performed three set of contrasts: Familiar Face vs Scrambled Face, Unfamiliar Face vs Scrambled Face, Familiar Face vs Unfamiliar Face. For each contrast, the null-distribution of the *t* statistic was constructed using 5000 permutation of the data, and the resulting *p*-values were corrected using the Benjamini and Hochberg's procedure (1995) to control the false discovery rate to address the problem of multiple comparisons. Furthermore, to minimize the risk of finding significant effects due to short-lived random fluctuations in a metric time-series, we deemed an effect as significant only when observed for at least 10 consecutive sampling points. Statistical analyses were performed using custom scripts developed in R (v. 3.5.5).

The same statistical approach was adopted to test the presence of difference in the event-related alpha power among the experimental conditions. For the same three set of contrasts described above, we performed a paired permutation-based *t*-test on the ERS/D data, averaged in 8–13 Hz range, correcting the resulting *p*-values using the Benjamini and Hochberg's procedure (1995) to control the false discovery rate. The analysis was performed in MATLAB using Brainstorm.

For what concerns the statistical testing of classification accuracy, we estimated for each time point the null distribution of the decoder performance. This distribution was generated by simulating 10000 time the decoding, for each time point following the same cross-validation scheme described above (Etzel, 2015), under the null hypothesis that the classification is performed by a random guess of the two categories. This distribution was then used to assess the probability to observe by chance a classification accuracy larger than the one obtain by the trained classifier.

### 3. Results

To model the evolution of functional connectivity during face processing, we reconstructed for each trial the source activity from MEG recordings. We first downsampled the source activity to the 148 nodes comprised in the Destrieux parcellation, and then computed the time-

resolved phase-locking value in the  $\alpha$  band. This resulted in a time series of connectivity matrices, representing the strength of connection between every nodes pair at each time-point (Fig. 1). These matrices were modeled as a time evolving graph, which was described in term of its global efficiency, compactness and entropy.

#### 3.1. Time-resolved evolution of network efficiency during face processing

We first wanted to test if face processing prompts an increased efficiency in the network compared to a scrambled image. Furthermore, we were interested in testing if familiarity with faces modulates this dynamic, and when this modulation does occur. Permutation based non-parametric analysis revealed that, for both global efficiency and network compactness, the network evolves in the hypothesized direction. The analyses showed that in an early time window, for both famous ( $t_{\max} = 164.67$ ,  $p < .05$ ) and unfamiliar ( $t_{\max} = 107.61$ ,  $p < .05$ ) faces the network diameter is reduced, leading to a shrinking of the network dimension, which becomes more compact (Fig. 2A, first and second panels). Conversely, in the same time window the global efficiency increases in response to both famous ( $t_{\max} = 129.73$ ,  $p < .05$ ) and unfamiliar ( $t_{\max} = 97.35$ ,  $p < .05$ ) faces when compared to scrambled faces (Fig. 2B, first and second panels). The analysis also revealed that around 300 ms, network diameter increases (i.e., the network becomes less compact) and global efficiency decreases for the contrast Famous vs Scrambled. With regard to the contrast between famous and unfamiliar faces, it revealed that during the processing of an unfamiliar face the network becomes, in a late time window, more compact ( $t_{\max} = 66.74$ ,  $p < .05$ , Fig. 2A third panel) and has more global efficiency ( $t_{\max} = 50.11$ ,  $p < .05$ , Fig. 2B third panel) compared to its shape during the processing of famous faces.

#### 3.2. Time-resolved evolution of network entropy during face processing

Having established that the network undergoes a dynamical reshaping of its connections in order to maximize its efficiency, we wanted to understand if this reshaping results in an increased network complexity. In the context of information theory, complexity can be defined in terms of Shannon Entropy, a statistical measure of how predictable the information content of a signal is. If the predictability is low, then the information conveyed by that signal is high and its entropy increases. In this study, the time-evolving predictability of network connections was used to quantify its entropy, hypothesizing that the dynamical rearranging of connectivity during face processing will result in an increased entropy of the system. Permutation based non-parametric analysis revealed that in an early time window, entropy increases in response to faces compared to scrambled images, peaking around 170 ms (Fig. 3, first and second panels). This effect was observed for both famous ( $t_{\max} = 135.71$ ,  $p < .05$ ) and unfamiliar faces ( $t_{\max} = 118.33$ ,  $p < .05$ ). Additionally, the contrast Famous vs Scrambled revealed a significant effect in a late time window, showing a reduction in network entropy for famous faces compared to scrambled images.

The analysis testing the difference in entropy between famous and



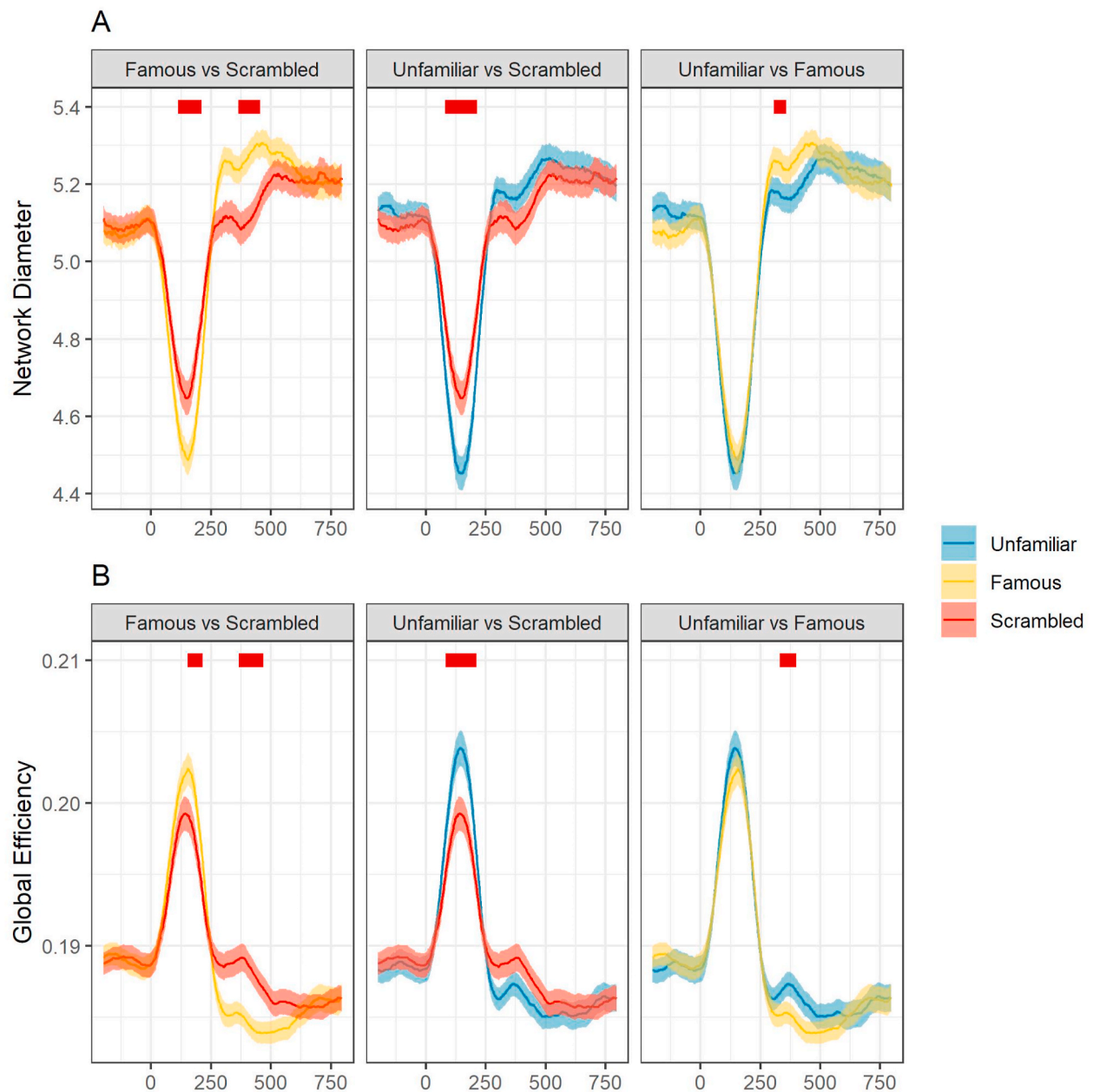


**Fig. 2.** Time-series of network diameter (A) and global efficiency (B). Each panel refers to a different contrast. The red ribbon on top of each panel indicates time frames in which a significant difference between categories was observed.

unfamiliar faces revealed a significant effect ( $t_{\max} = 65.47$ ,  $p < .05$ ) occurring around 300 ms, showing that entropy is larger when the processed face is unfamiliar (Fig. 3, third panel).

### 3.3. Routing efficiency between the core and the extended systems

Face processing relies on the activity of distributed set of cortical regions that comprise the *face processing* network. We wanted to model this activity, with a specific focus on the cross-communication among the nodes in the *core* system and the nodes in the *extended* system. This cross-communication was quantified in terms of how efficiently the information is routed between the two systems. Permutation-based non parametric analysis revealed that in response to a face the information flow between them becomes rapidly more efficient, with a peak around 170 ms. This effect has been observed for both famous ( $t_{\max} = 114.85$ ,  $p < .05$ ) and unfamiliar faces ( $t_{\max} = 253.29$ ,  $p < .05$ ) compared to scrambled faces (Fig. 4, first and second panels). Additionally, we

observed only for unfamiliar faces that routing efficiency increases also in a late time window (Fig. 4, second panel).

With regard to the Famous vs Unfamiliar contrast (Fig. 4, third panel), the analysis revealed a significant effect showing that routing efficiency is larger when the face under processing is unfamiliar ( $t_{\max} = 43.42$ ,  $p < .05$ ).

### 3.4. Time-resolved decoding of familiarity from connectivity patterns

The analysis of network topological changes and cross-talk among the nodes of the face perception network are sensitive to face familiarity. In order to probe the connectivity dynamics subtending the extraction of this abstract feature, we applied multivariate pattern recognition on the time-resolved connectivity estimated during processing of famous and unfamiliar faces. The decoder showed an above chance classification accuracy ( $p < .05$ ) as early as  $\sim 100$  ms (Fig. 5C), confirming that familiarity is a feature that is extracted very rapidly from the stimulus.

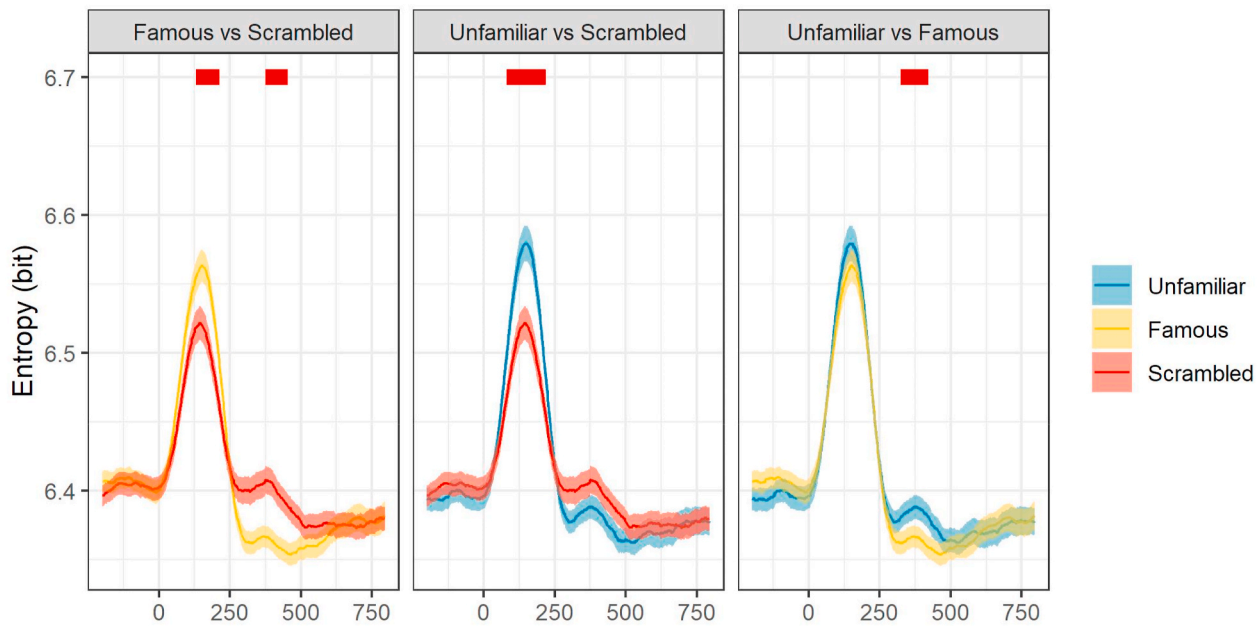


**Fig. 3.** Time-series of network entropy. Each panel refers to a different contrast. The red ribbon on top of each panel indicates time frames in which a significant difference between categories was observed.

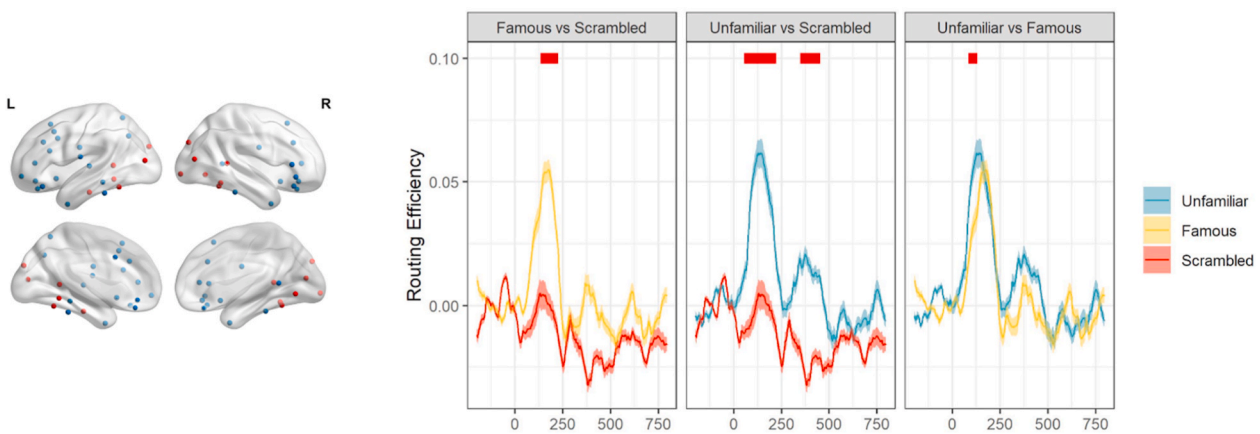


**Fig. 4.** Time-series of routing efficiency between the *core* (red nodes) and the *extended* (blue nodes) systems. Each panel refers to a different contrast. The red ribbon on top of each panel indicates time frames in which a significant difference between categories was observed.

Projecting the classifier weights in the original connectivity space (Fig. 5D), we reveal that this extraction relies on two connection pathways, mainly in right hemisphere, that grant communication between posterior and anterior nodes of the face perception network. A more ventral pathway that connects extrastriate visual cortices to anterior regions, like the inferior frontal gyrus and the anterior insula, and a dorsal pathway that projects the information to parietal associative cortices (inferior parietal cortex and precuneus) through the superior temporal sulcus. Furthermore, this analysis reveals that a fine-grained processing of the face relies on many different nodes that do not usually show a face-selective response in standard univariate activation-based analysis (i.e. GLM and ERP/ERF). The pattern we observed is also in line with a recent study employing MVPA on fMRI activation to familiar and unfamiliar faces (Visconti Di Oleggio Castello et al., 2017). In this study the authors identified a larger set of regions contributing to the cortical representation of familiarity, comprising portions of the face perception system that with GLM-based analysis fail to show an association with familiarity extraction. Overall, this suggests that face processing might be more distributed than how current theoretical models

envision (Bernstein and Yovel, 2015; Duchaine and Yovel, 2015).

### 3.5. Analysis of event-related power changes in the alpha band

A recent study (Demuru et al., 2020) showed that changes in the oscillatory power of a node activity, unrelated to its connectivity with other nodes in the network, might bias the graph-theoretical analysis of networks estimated from electrophysiological measures of cortical connectivity.

Although this bias has been reported for nodal measures, rather than global network properties like the one investigated in this study, we wanted to rule out this possibility. Indeed, analysis of event-related modulation of oscillatory power in the alpha band did not show any differences among the experimental conditions (Fig. 6). This result is important because it shows that our network modeling approach is effective in tracking the inter-regional time and phase-locked communication in the alpha band, ruling out potential confounds related to underlying alpha power modulations.

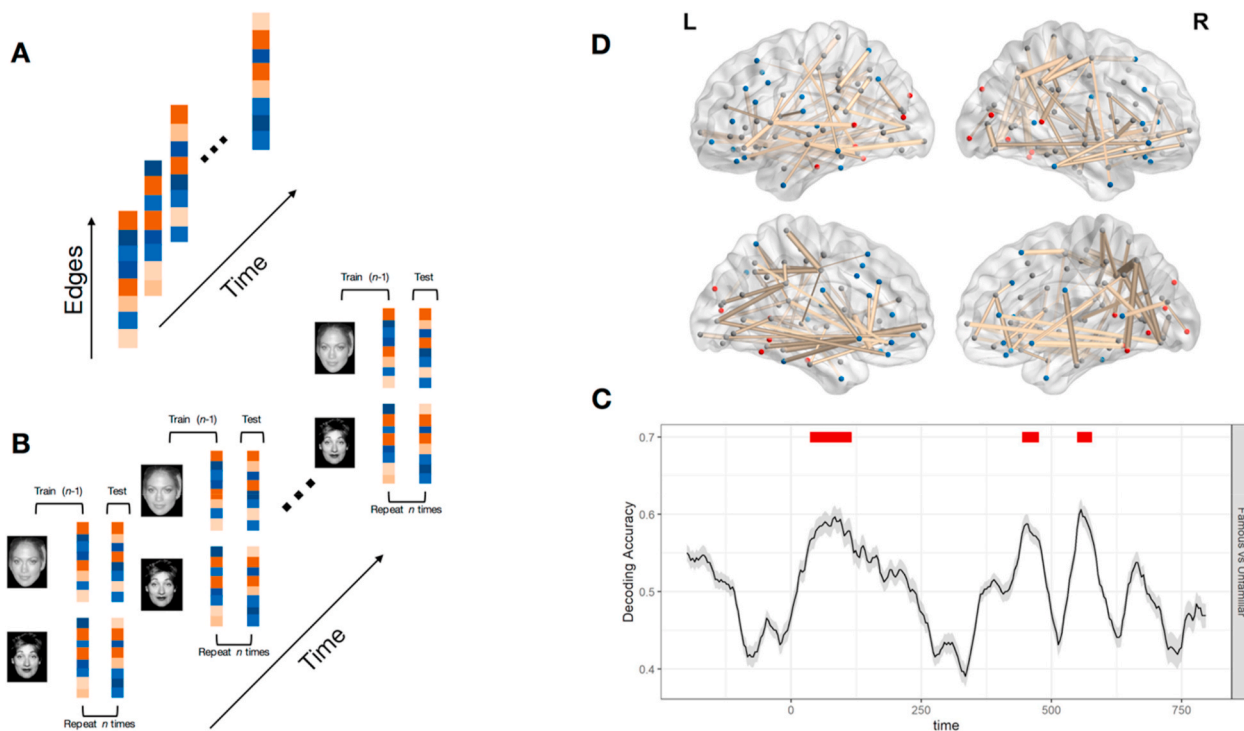


Fig. 5. Time-resolved decoding of face familiarity. After vectorization of connectivity patterns (A), decoding analysis of famous and unfamiliar faces was performed at each time point using a leave-one-subject out cross-validation scheme (B). Significant time frames of decoding accuracy are highlighted by the red ribbon (C). Classifier weights were projected in the original connectivity space to highlight the most critical edges for extracting face familiarity (D).

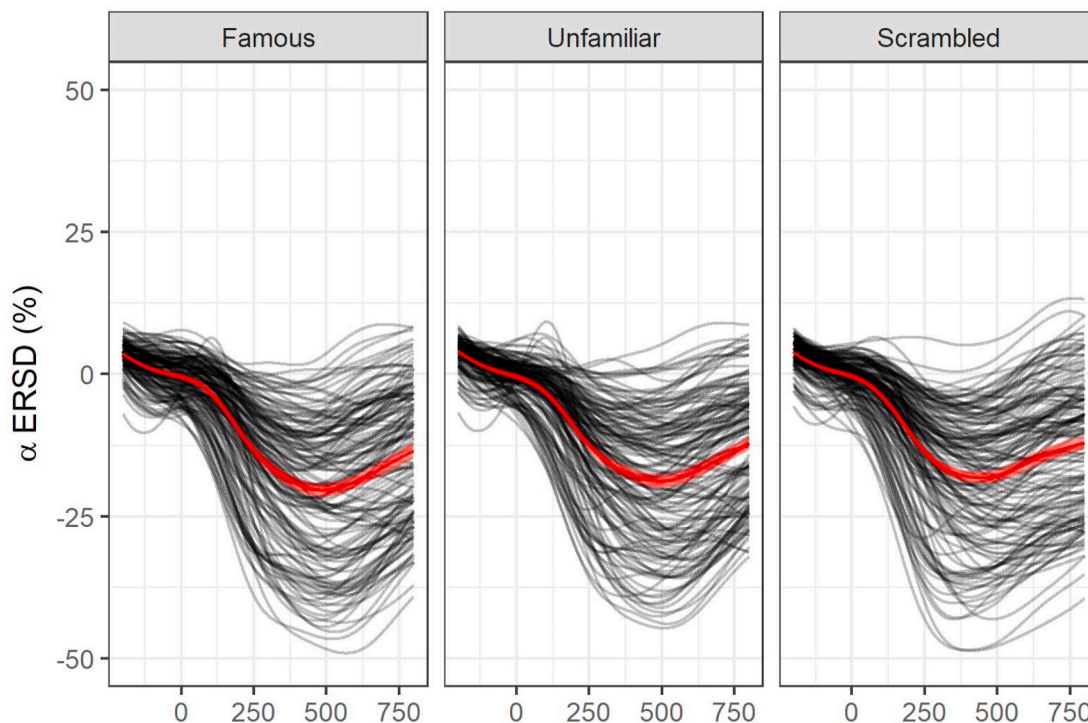


Fig. 6. Butterfly plots showing the grand average event-related desynchronization in the alpha band for each stimulus category. The black lines represent each ROI, the red lines represent the grand mean surrounded by shaded ribbons representing the standard errors.

### 3.6. Correlation of event-related fields and event-related network changes

The results presented so far show that strong event-related topological changes characterize the cortical network in the time-windows in

which the typical face-evoked potentials occur. In order to rule out the possibility that the dynamics observed in the network are not simply a redundant way to present information already contained in the event-related fields, we correlated the latter with each network metric time-

series. Additionally, we computed the correlation among the network metrics time series, in order to understand how much each metric represents unique information.

We found that the median correlations and the shared variance between our network metrics and the grand-average event-related field, for each stimulus category, were very modest (ranging from 0 to 0.12, top row of Fig. 7). Similar patterns were observed when correlating network metrics time-series with the event-related fields of each ROI (Supplementary Fig. 1). Additionally, to investigate the robustness of our results, we also performed the statistical contrasts described in the previous sections after regressing out the event-related field time-series from the network metric time-series, showing that the results are unchanged (Supplementary Fig. 2). Altogether, the results of these analyses suggest that the metrics used in this study carry unique information regarding the state of the network during face processing.

With regards to the correlations among the network metrics, the results show that some are strongly correlated among them (Fig. 7). Specifically, we found a strong negative correlation between the Diameter and the Global Efficiency ( $r = 0.98$ ). This is not surprising, since these two metrics are both computed from the network path length (see Methods) and show, from different perspectives, the same underlying network dynamic, that is the network shrinking leading to a higher efficiency in sharing information. We observed that these two metrics are also strongly correlated with Entropy. This is an interesting result, because it shows that Entropy, on one side, and Diameter and Global efficiency on the other, are tracking a coherent modulation of the connectivity weights defining the network, despite being derived through completely different computations. Finally, we observed very modest correlations with the fourth metric that we used, that is the Routing efficiency. This is an important result, because this latter metric was designed to track the dynamics only within the nodes comprising the face processing network. Observing that it has very modest correlation with the metrics that measure whole-brain topological changes support

the claim that using different metrics is necessary to highlight different and non-redundant features of the network dynamical reshaping that supports face processing.

#### 4. Discussion

The present paper focused on the investigation of event-related changes in the cortical network measured with MEG during a simple face processing task. The aim of this research was twofold. First, it sought to understand, on the fine temporal scale provided by MEG, the dynamic changes that brain networks go through when probed with a task. Second, it aimed at showing how the investigation of cortical connectivity can improve our understanding of the neuro-cognitive mechanisms underlying face processing. To accomplish these goals, we first estimated the time-varying phase synchronization among 148 cortical regions in the alpha band, which has been proved to be the cortical oscillatory mode most sensitive to the activity of large scale brain networks (Samogin et al., 2020). Then, we computed a series of graph-theoretical measures to characterize how network topology, efficiency and complexity changed in time as a function of the features of the target stimulus.

With regard to the first aim, we found that during face processing the cortical network undergoes a series of substantial changes, in terms of its complexity, topological shape, and efficiency of information flow, unfolding in a coherent timing. Comparing the dynamic elicited by a face with the one elicited by a scrambled image, we observed an increase in the information entropy of the network together with a reduction of its diameter and an increase of its global efficiency. This pattern of changes suggests that, when probed with a visual stimulus, the cortical network adapts its connections to maximize the encoding and the successful processing of the stimulus itself, especially when it has an inherent meaning, as it is the case with the image of a face.

Functional MRI investigation of the time-evolving modularity of

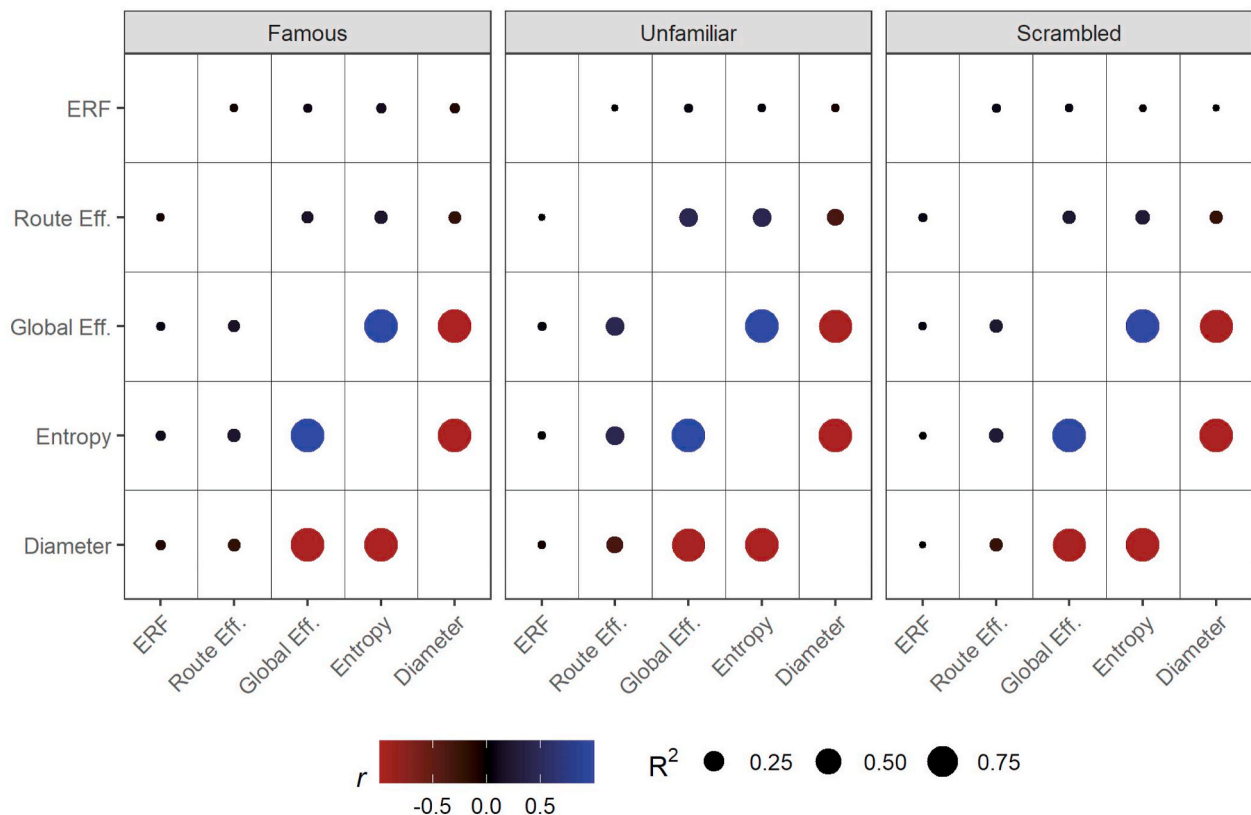


Fig. 7. Median correlations and shared variance between each network time series and grand-average event related fields, separately for each condition.



brain network already established that cognitive activity is mediated by a dynamic reconfiguration of network topology. These studies showed that a task-induced reshaping of the network modular structure occurs recurrently on several time scales, from days to seconds (Bassett et al., 2011, 2015, 2011; Shine et al., 2016). This reshaping is thought to serve mainly one purpose, that is maximizing integration across heterogeneous regions, at the cost of segregation, in order to prioritize the execution of cognitive demanding processes (Shine et al., 2016). Moreover, we recently extended these findings, demonstrating that similar dynamics can be detected also on the finer temporal scale provided by EEG (Maffei and Sessa, 2021).

The present results further improve our understanding of how the network topology changes when it is probed with a task. The dynamic readjustment in the connectivity pattern translates to a reduction of the overall diameter of the network, that becoming more compact is characterized by an easier information exchange across its nodes. This is shown by the concomitant increase in the global efficiency of the network, a metric that quantifies how efficient is the information flow in the network. As a consequence of this topological readjustment, the pattern of connections among the cortical regions become more complex, as shown by an increase in the Shannon entropy of the network. This increase suggests that the information stored in the network edges becomes less predictable during the processing of a stimulus, so its density increases. This latter result seems appealing also because it is in line with a series of converging evidence that, leveraging the concept of entropy, suggest that the brain operates in a non-equilibrium state characterized by an increased entropy, especially when probed with cognitive demanding tasks (Lynn et al., 2020; Viol et al., 2017).

Interestingly, we detected these coordinated event-related network changes in a time-window comprised between 100 and 200 ms, observing also that they are characterized by a peak around 170 ms. This time-evolving pattern closely follows the typical timing observed in the well-established event-related potentials/event-related fields elicited by face processing, characterized by a component with a negative polarity and a peak latency around 170 ms. These results, focusing on whole-brain connectivity, rather than on the local activation detected by ERP/ERF, have the potential to shed new light regarding the mechanisms that ultimately give rise to the typical event-related response. Indeed, this response can be thought as the final output of an underlying process of elaboration that operates through phase synchronization of firing from disparate neural populations (Nunez, 2000; Nunez and Srinivasan, 2006). These results, tracking this underlying dynamic, suggest that a fast and large-scale rearrangement of the functional network, in terms of its shape and efficiency, is strongly associated with the event-related modulation of the cortical potential. This adds to several previous studies highlighting a relationship between the ERP response and the time-evolving phase synchronization across the whole cortical network (Dimitriadis et al., 2013; Karamzadeh et al., 2013; Martini et al., 2012).

With regard to its second aim, this research provides several interesting insights about the network dynamics that subtend face processing and how familiarity affects its elaboration. We observed modulations of the network state in two different time-windows. In an early *face-sensitive* window, we observed for both famous and unfamiliar faces a similar pattern of response of increased efficiency compared to scrambled images. Furthermore, studying the information flow between the *core* and the *extended* systems of the face processing network revealed an interesting pattern in their cross-communication. In the first 200 ms the topological distance between the two systems is dramatically reduced when processing a face compared to a scrambled image. Altogether these results fit nicely with studies suggesting that face encoding occurs through a bidirectional communication between early visual areas and higher-order regions comprising the face perception network (Rossion, 2014; Wang et al., 2020; Zhao et al., 2018). In addition, they reveal the topological dynamic of this process in terms of both the whole cortical network and the specific subsets of nodes involved in face processing.

For what concerns the effect of familiarity, an open question is when this information is extracted. Scalp electrophysiology suggests that the effect of familiarity can be detected not earlier than 250 ms, but this result has been questioned by recent behavioral and neuroimaging evidence showing that face identity is extracted earlier (Dobs et al., 2019; Visconti di Oleggio Castello and Gobbini, 2015). Our results provide the ground to reconcile this apparent discrepancy. Indeed, we observed that it is possible to decode familiarity information from connectivity patterns as early as  $\sim 100$  ms. Then, in a later time window, we observe that when the network is processing a face with an unknown identity it maintains the task-induced configuration. Conversely, when the face is known it returns to its resting topology. Our interpretation of this result is that, in the first stage of processing the network reshapes to maximize its efficiency and to support information exchange between the core and the extended systems. This dynamic is needed in order to establish a positive match between the incoming information and the stored one (Apps and Tsakiris, 2013; Trapp et al., 2018). This pattern-matching happens through a similar reshaping of the functional network, for both familiar and unfamiliar faces, as we did not observe difference between the two in the early time frame in terms of global topology. We also observed that the information flow between the core and extended systems increased similarly for both, with a slightly increased efficiency for the latter. Then, when the positive match occurs for a famous face, the network returns to an idling state because maintaining that network configuration would likely require unnecessary metabolic costs (Achard and Bullmore, 2007; Bassett and Bullmore, 2006; Bullmore and Sporns, 2012; Lynn et al., 2020). This is supported by the results showing a drop in all the global topological metrics investigated. Instead, when the face under processing is unknown no match could have taken place in the early time window, therefore the core and extended system have to maintain an efficient cross-talk, likely based on the refined information available after the full encoding of the visual features of the face has been completed.

## 5. Conclusions

This research provides new insights regarding the time-evolving properties of brain networks, showing that cognitive tasks induce a reshaping of the network topology which is rapid and coordinated. The consistency observed across the metrics investigated suggests that this dynamic readjustment has the ultimate goal to maximize the efficiency of the communication pathways across cortical nodes. Furthermore, the timing features of this dynamics highlight the inherent potential that investigating event-related network changes has for understanding the timing of cognitive operations. Indeed, these results provide an empirical evidence of the predicted cross-systems information exchange underlying face processing.

Altogether, this adds to the flourishing field of functional *chronnectomics* (Calhoun et al., 2014; Preti et al., 2017) and calls for further investigation of network dynamics using electrophysiological estimates of cortical connectivity. Indeed, this study does not come without limitations that should be addressed in future studies. First, in this study we focused on alpha band because it is strongly related with the activity of large-scale cortical networks and because face processing is related with alpha phase connectivity. Nevertheless, recent studies, characterizing the resting-state functional networks with a multi-spectral resolution approach, suggested that the network architecture can be also the results of interactions between oscillations with different frequencies (Iandolo et al., 2020; Samogin et al., 2020). Thus, future research should aim at extending the present findings to characterize in detail how these interactions evolve in time during a task. Second, future works should aim at extending the current results to different experimental tasks, like an active face recognition task, in order to detail further the unfolding of network activity underlying face processing. Third, it would be ideal to also characterize the network dynamics contrasting face-evoked activity to both a scrambled face and a different stimulus category, to gain a

more comprehensive understanding of what the face-specific dynamics are.

Finally, it is also important to stress the limits of the decoding analysis used. First, we observed that the classification yielded moments of below-chance accuracy which has been previously suggested as a drawback of low SNR in the data features (Jamalabadi et al., 2016). This does not invalidate the results observed, whose significance has been assessed using permutations (Etzel, 2015; Jamalabadi et al., 2016), but nevertheless invites to for further investigations to evaluate their generalizability. Second, our connectivity estimate was not at the single-trial level therefore we could not employ different cross-validation schemes to disentangle the contribution of familiarity from identity and low-level image features (Visconti Di Oleggio Castello et al., 2017).

### Declaration of competing interests

The authors declare that they have no known competing financial interests or personal relationships that could have appeared to influence the work reported in this paper.

### Funding

No specific funding supported the research presented in this manuscript.

### CRedit authorship contribution statement

**Antonio Maffei:** Conceptualization, Data curation, Methodology, Formal analysis, Visualization, Writing - original draft. **Paola Sessa:** Conceptualization, Supervision, Writing - review & editing.

### Appendix A. Supplementary data

Supplementary data to this article can be found online at <https://doi.org/10.1016/j.yinrp.2021.100022>.

### References

- Achard, S., Bullmore, E., 2007. Efficiency and cost of economical brain functional networks. *PLoS Comput. Biol.* 3, e17. <https://doi.org/10.1371/journal.pcbi.0030017>.
- Apps, M.A.J., Tsakiris, M., 2013. Predictive codes of familiarity and context during the perceptual learning of facial identities. *Nat. Commun.* 4, 1–10. <https://doi.org/10.1038/ncomms3698>.
- Bahramisharif, A., van Gerven, M.A.J., Aarnoutse, E.J., Mercier, M.R., Schwartz, T.H., Foxe, J.J., Ramsey, N.F., Jensen, O., 2013. Propagating neocortical gamma bursts are coordinated by traveling alpha waves. *J. Neurosci.* 33, 18849–18854. <https://doi.org/10.1523/JNEUROSCI.2455-13.2013>.
- Bassett, D.S., Bullmore, E., 2006. Small-world brain networks. *Neuroscientist*. <https://doi.org/10.1177/1073858406293182>.
- Bassett, D.S., Bullmore, E.T., Meyer-Lindenberg, A., Apud, J.A., Weinberger, D.R., Coppola, R., 2009. Cognitive Fitness of Cost-Efficient Brain Functional Networks. *PNAS July*.
- Bassett, D.S., Wymbs, N.F., Porter, M.A., Mucha, P.J., Carlson, J.M., Grafton, S.T., 2011. Dynamic reconfiguration of human brain networks during learning. *Proc. Natl. Acad. Sci. U. S. A.* 108, 7641–7646. <https://doi.org/10.1073/pnas.1018985108>.
- Bassett, D.S., Yang, M., Wymbs, N.F., Grafton, S.T., 2015. Learning-induced autonomy of sensorimotor systems. *Nat. Neurosci.* 18, 744–751. <https://doi.org/10.1038/nn.3993>.
- Benjamini, Y., Hochberg, Y., 1995. Benjamini-1995.pdf. *J. Roy. Stat. Soc. B*. <https://doi.org/10.2307/2346101>.
- Bernstein, M., Yovel, G., 2015. Two neural pathways of face processing: a critical evaluation of current models. *Neurosci. Biobehav. Rev.* 55, 536–546. <https://doi.org/10.1016/j.neubiorev.2015.06.010>.
- Bola, M., Sabel, B.A., 2015. Dynamic reorganization of brain functional networks during cognition. *Neuroimage* 114, 398–413. <https://doi.org/10.1016/j.neuroimage.2015.03.057>.
- Bullmore, E., Sporns, O., 2012. The economy of brain network organization. *Nat. Rev. Neurosci.* <https://doi.org/10.1038/nrn3214>.
- Bullmore, E., Sporns, O., 2009. Complex brain networks: graph theoretical analysis of structural and functional systems. *Nat. Rev. Neurosci.* <https://doi.org/10.1038/nrn2575>.
- Calhoun, V.D., Miller, R., Pearlson, G., Adali, T., 2014. The chronnectome: time-varying connectivity networks as the next frontier in fMRI data discovery. *Neuron*. <https://doi.org/10.1016/j.neuron.2014.10.015>.
- Demuru, M., La Cava, S.M., Pani, S.M., Fracchini, M., 2020. A comparison between power spectral density and network metrics: an EEG study. *Biomed. Signal Process. Contr.* 57, 101760. <https://doi.org/10.1016/j.bspc.2019.101760>.
- Dimitriadis, S.I., Laskaris, N.A., Tzelepi, A., 2013. On the quantization of time-varying phase synchrony patterns into distinct functional connectivity microstates (FCstates) in a multi-trial visual ERP paradigm. *Brain Topogr.* 26, 397–409. <https://doi.org/10.1007/s10548-013-0276-z>.
- Dobs, K., Isik, L., Pantazis, D., Kanwisher, N., 2019. How face perception unfolds over time. *Nat. Commun.* 10, 1–10. <https://doi.org/10.1038/s41467-019-09239-1>.
- Duchaine, B., Yovel, G., 2015. A revised neural framework for face processing. *Annu. Rev. Vis. Sci.* 1, 393–416. <https://doi.org/10.1146/annurev-vision-082114-035518>.
- Eimer, M., 2012. The face-sensitive N170 component of the event-related brain potential. *Oxford Handbook of Face Perception*. <https://doi.org/10.1093/oxfordhb/9780199559053.013.0017>.
- Etzel, J.A., 2015. MVPA permutation schemes: permutation testing for the group level. *Proceedings - 2015 International Workshop on Pattern Recognition in NeuroImaging, PRNI 2015*. Institute of Electrical and Electronics Engineers Inc., pp. 65–68. <https://doi.org/10.1109/PRNI.2015.29>.
- Gi, X., Bae, Y., Luck, S.J., 2018. Dissociable Decoding of Spatial Attention and Working Memory from EEG Oscillations and Sustained Potentials. <https://doi.org/10.1523/JNEUROSCI.2860-17.2017>.
- Groetswagers, T., Wardle, S.G., Carlson, T.A., 2017. Decoding dynamic brain patterns from evoked responses: a tutorial on multivariate pattern analysis applied to time series neuroimaging data. *J. Cognit. Neurosci.* 29, 677–697. <https://doi.org/10.1162/jocn.a.01068>.
- Groppe, D.M., Urbach, T.P., Kutas, M., 2011. Mass univariate analysis of event-related brain potentials/fields I: a critical tutorial review. *Psychophysiology*. <https://doi.org/10.1111/j.1469-8986.2011.01273.x>.
- Haufe, S., Meinecke, F., Görden, K., Dähne, S., Haynes, J.D., Blankertz, B., Bießmann, F., 2014. On the interpretation of weight vectors of linear models in multivariate neuroimaging. *Neuroimage* 87, 96–110. <https://doi.org/10.1016/j.neuroimage.2013.10.067>.
- Haxby, J.V., Gobbini, M.I., 2012. Distributed Neural Systems for Face Perception. In: *Oxford Handbook of Face Perception*, pp. 93–110. <https://doi.org/10.1093/oxfordhb/9780199559053.013.0006>.
- Haxby, J.V., Hoffman, E.A., Gobbini, M.I., 2000. The distributed human neural system for face perception. *Trends Cognit. Sci.* [https://doi.org/10.1016/S1364-6613\(00\)01482-0](https://doi.org/10.1016/S1364-6613(00)01482-0).
- Hoffman, E.A., Gobbini, M.I., Haxby, J.V., 2002. Human neural systems for face recognition and social communication. *Biol. Psychiatr.* 51, 59–67.
- Huang, W., Wu, X., Hu, L., Wang, L., Ding, Y., Qu, Z., 2017. Revisiting the earliest electrophysiological correlate of familiar face recognition. *Int. J. Psychophysiol.* 120, 42–53. <https://doi.org/10.1016/j.ijpsycho.2017.07.001>.
- Iandolo, R., Semprini, M., Mantini, D., Buccelli, S., Sona, D., Avanzino, L., Chiappalone, M., 2020. Frequency-specific meso-scale structure of spontaneous oscillatory activity in the human brain. *bioRxiv*, 114488. <https://doi.org/10.1101/2020.05.26.114488>, 2020.05.26.
- Jamalabadi, H., Alizadeh, S., Schönauer, M., Leibold, C., Gais, S., 2016. Classification based hypothesis testing in neuroscience: below-chance level classification rates and overlooked statistical properties of linear parametric classifiers. *Hum. Brain Mapp.* 37, 1842–1855. <https://doi.org/10.1002/hbm.23140>.
- Jerbi, K., Ossandón, T., Hamamé, C.M., Senova, S., Dalal, S.S., Jung, J., Minotti, L., Bertrand, O., Berthoz, A., Kahane, P., Lachaux, J.P., 2009. Task-related gamma-band dynamics from an intracerebral perspective: review and implications for surface EEG and MEG. *Hum. Brain Mapp.* 30, 1758–1771. <https://doi.org/10.1002/hbm.20750>.
- Karamzadeh, N., Medvedev, A., Azari, A., Gandjbakhche, A., Najafizadeh, L., 2013. Capturing dynamic patterns of task-based functional connectivity with EEG. *Neuroimage* 66, 311–317. <https://doi.org/10.1016/j.neuroimage.2012.10.032>.
- Lynn, C.W., Cornblath, E.J., Papadopoulos, L., Bertolero, M.A., Bassett, D.S., 2020. Non-equilibrium Dynamics and Entropy Production in the Human Brain.
- Maffei, A., 2020. Spectrally resolved EEG intersubject correlation reveals distinct cortical oscillatory patterns during free-viewing of affective scenes. *Psychophysiology*. <https://doi.org/10.1111/psyp.13652>.
- Maffei, A., Polver, S., Spironelli, C., Angrilli, A., 2020. EEG gamma activity to emotional movies in individuals with high traits of primary “successful” psychopathy. *Brain Cognit.* 143. <https://doi.org/10.1016/j.bandc.2020.105599>.
- Maffei, A., Sessa, P., 2021. Event-related network changes unfold the dynamics of cortical integration during face processing. *Psychophysiology* 1–16. <https://doi.org/10.1111/psyp.13786>.
- Maffei, A., Spironelli, C., Angrilli, A., 2019. Affective and cortical EEG gamma responses to emotional movies in women with high vs low traits of empathy. *Neuropsychologia* 133, 107175. <https://doi.org/10.1016/j.neuropsychologia.2019.107175>.
- Mantini, D., Perrucci, M.G., Del Gratta, C., Romani, G.L., Corbetta, M., Raichle, M.E., 2007. Electrophysiological Signatures of Resting State Networks in the Human Brain.
- Maris, E., Oostenveld, R., 2007. Nonparametric statistical testing of EEG- and MEG-data. *J. Neurosci. Methods* 164, 177–190. <https://doi.org/10.1016/j.jneumeth.2007.03.024>.
- Martini, N., Menicucci, D., Sebastiani, L., Bedini, R., Pingitore, A., Vanello, N., Milanese, M., Landini, L., Gemignani, A., 2012. The dynamics of EEG gamma responses to unpleasant visual stimuli: from local activity to functional connectivity. *Neuroimage* 60, 922–932. <https://doi.org/10.1016/j.neuroimage.2012.01.060>.

- Massimini, M., Huber, R., Ferrarelli, F., Hill, S., Tononi, G., 2004. The sleep slow oscillation as a traveling wave. *J. Neurosci.* 24, 6862–6870. <https://doi.org/10.1523/JNEUROSCI.1318-04.2004>.
- Muller, L., Chavane, F., Reynolds, J., Sejnowski, T.J., 2018. Cortical travelling waves: mechanisms and computational principles. *Nat. Rev. Neurosci.* <https://doi.org/10.1038/nrn.2018.20>.
- Nobukawa, S., Kikuchi, M., Takahashi, T., 2019. Changes in functional connectivity dynamics with aging: a dynamical phase synchronization approach. *Neuroimage* 188, 357–368. <https://doi.org/10.1016/j.neuroimage.2018.12.008>.
- Nunez, P.L., 2000. Toward a quantitative description of large-scale neocortical dynamic function and EEG. *Behav. Brain Sci.* 23 <https://doi.org/10.1017/S0140525X00003253>.
- Nunez, P.L., Srinivasan, R., 2006. A theoretical basis for standing and traveling brain waves measured with human EEG with implications for an integrated consciousness. *Clin. Neurophysiol.* 117, 2424–2435. <https://doi.org/10.1016/j.clinph.2006.06.754>.
- Pedersen, M., Omidvarnia, A., Zalesky, A., Jackson, G.D., 2018. On the relationship between instantaneous phase synchrony and correlation-based sliding windows for time-resolved fMRI connectivity analysis. *Neuroimage* 181, 85–94. <https://doi.org/10.1016/j.neuroimage.2018.06.020>.
- Preti, M.G., Bolton, T.A., Van De Ville, D., 2017. The dynamic functional connectome: state-of-the-art and perspectives. *Neuroimage* 160, 41–54. <https://doi.org/10.1016/j.neuroimage.2016.12.061>.
- Ramon, M., Gobbini, M.I., 2018. Familiarity matters: a review on prioritized processing of personally familiar faces. *Vis. cogn.* 26, 179–195. <https://doi.org/10.1080/13506285.2017.1405134>.
- Rossion, B., 2014. Understanding face perception by means of human electrophysiology. *Trends Cognit. Sci.* <https://doi.org/10.1016/j.tics.2014.02.013>.
- Rubinov, M., Sporns, O., 2010. Complex network measures of brain connectivity: uses and interpretations. *Neuroimage* 52, 1059–1069. <https://doi.org/10.1016/j.neuroimage.2009.10.003>.
- Sadaghiani, S., Scheeringa, R., Lehongre, K., Morillon, B., Giraud, A.L., Kleinschmidt, A., 2010. Intrinsic connectivity networks, alpha oscillations, and tonic alertness: a simultaneous electroencephalography/functional magnetic resonance imaging study. *J. Neurosci.* 30, 10243–10250. <https://doi.org/10.1523/JNEUROSCI.1004-10.2010>.
- Samogin, J., Marino, M., Porcaro, C., Wenderoth, N., Dupont, P., Swinnen, S.P., Mantini, D., 2020. Frequency-dependent functional connectivity in resting state networks. *Hum. Brain Mapp. hbm.* 25184 <https://doi.org/10.1002/hbm.25184>.
- Santaracchi, E., Galli, G., Polizzotto, N.R., Rossi, A., Rossi, S., 2014. Efficiency of weak brain connections support general cognitive functioning. *Hum. Brain Mapp.* 35, 4566–4582. <https://doi.org/10.1002/hbm.22495>.
- Shine, J.M., Bissett, P.G., Bell, P.T., Koyejo, O., Balsters, J.H., Gorgolewski, K.J., Moodie, C.A., Poldrack, R.A., 2016. The dynamics of functional brain networks: integrated network states during cognitive task performance. *Neuron* 92, 544–554. <https://doi.org/10.1016/j.neuron.2016.09.018>.
- Steriade, M., McCormick, D.A., Sejnowski, T.J., 1993. Thalamocortical oscillations in the sleeping and aroused brain. *Science* 84 262, 679–685. <https://doi.org/10.1126/science.8235588>.
- Tadel, F., Baillet, S., Mosher, J.C., Pantazis, D., Leahy, R.M., 2011. Brainstorm: a user-friendly application for MEG/EEG analysis. *Comput. Intell. Neurosci.* 13. <https://doi.org/10.1155/2011/879716>, 2011.
- Tadel, F., Bock, E., Niso, G., Mosher, J.C., Cousineau, M., Pantazis, D., Leahy, R.M., Baillet, S., 2019. MEG/EEG group Analysis with Brainstorm. *Front. Neurosci.* 13, 76. <https://doi.org/10.3389/fnins.2019.00076>.
- Taylor, D., Shai, S., Stanley, N., Mucha, P.J., 2016. Enhanced detectability of community structure in multilayer networks through layer aggregation. *Phys. Rev. Lett.* 116, 228301. <https://doi.org/10.1103/PhysRevLett.116.228301>.
- Trapp, S., Schweinberger, S.R., Hayward, W.G., Kovács, G., 2018. Integrating predictive frameworks and cognitive models of face perception. *Psychon. Bull. Rev.* <https://doi.org/10.3758/s13423-018-1433-x>.
- Valencia, M., Martinerie, J., Dupont, S., Chavez, M., 2008. Dynamic small-world behavior in functional brain networks unveiled by an event-related networks approach. *Phys. Rev. E - Stat. Nonlinear Soft Matter Phys.* 77 <https://doi.org/10.1103/PhysRevE.77.050905>.
- van Driel, J., Knäpen, T., van Es, D.M., Cohen, M.X., 2014. Interregional alpha-band synchrony supports temporal cross-modal integration. *Neuroimage* 101, 404–415. <https://doi.org/10.1016/j.neuroimage.2014.07.022>.
- Viol, A., Palhano-Fontes, F., Onias, H., De Araujo, D.B., Viswanathan, G.M., 2017. Shannon entropy of brain functional complex networks under the influence of the psychedelic Ayahuasca. *Sci. Rep.* 7, 1–13. <https://doi.org/10.1038/s41598-017-06854-0>.
- Visconti di Oleggio Castello, M., Gobbini, M.I., 2015. Familiar face detection in 180ms. *PLoS One* 10, e0136548. <https://doi.org/10.1371/journal.pone.0136548>.
- Visconti Di Oleggio Castello, M., Halchenko, Y.O., Guntupalli, J.S., Gors, J.D., Gobbini, M.I., 2017. The neural representation of personally familiar and unfamiliar faces in the distributed system for face perception. *Sci. Rep.* 7 <https://doi.org/10.1038/s41598-017-12559-1>.
- Wakeman, D.G., Henson, R.N., 2015. A multi-subject, multi-modal human neuroimaging dataset. *Sci. data* 2, 150001. <https://doi.org/10.1038/sdata.2015.1>.
- Wang, Y., Metoki, A., Smith, D.V., Medaglia, J.D., Zang, Y., Benear, S., Popal, H., Lin, Y., Olson, I.R., 2020. Multimodal mapping of the face connectome. *Nat. Hum. Behav.* 4, 397–411. <https://doi.org/10.1038/s41562-019-0811-3>.
- Yarkoni, T., Poldrack, R.A., Nichols, T.E., Van Essen, D.C., Wager, T.D., 2011. Large-scale automated synthesis of human functional neuroimaging data. *Nat. Methods* 8, 665–670. <https://doi.org/10.1038/nmeth.1635>.
- Zhao, Y., Zhen, Z., Liu, X., Song, Y., Liu, J., 2018. The neural network for face recognition: insights from an fMRI study on developmental prosopagnosia. *Neuroimage* 169, 151–161. <https://doi.org/10.1016/j.neuroimage.2017.12.023>.